Optical and Quantum Electronics (2023) 55:162
https://doi.org/10.1007/s11082-022-04437-6

Solitons in dual-core optical fibers with chromatic dispersion

Muslum Ozisik[1] · Mustafa Bayram[2] · Aydin Secer[1,2] · Melih Cinar[1]

Received: 31 October 2022 / Accepted: 27 November 2022 / Published online: 3 January 2023

Abstract
In this paper, some analytical solutions for a model of dual-core optical fibers governed by a system of coupled non-linear Schrödinger equations (NLSEs) and the effect of the coefficient of the group velocity dispersion term on the considered model are investigated. The group velocity dispersion (GVD) has a important role in the optical wave propagation. The enhanced modified extended tanh expansion method (eMETEM) is successfully implemented to the governing model. The NLSE system is turned into a nonlinear ordinary differential equation (NLODE) via appropriate wave transformations. Supposing that the NLODE has solutions in the form suggested by the method and utilizing the enhanced solutions of the Riccati equation, we gain a nonlinear system of algebraic equations. The solutions of the governing model are obtained after solving the system of algebraic equations. 2D, 3D and contour illustrative figures for the physical interpretation of the attained solutions are presented. Besides, the result of the investigation, which is related to the effect of the coefficient of the group velocity dispersion term, is presented by supporting the various graphical scheme.

Keywords Group velocity dispersion · Dual-core optical fibers · Soliton propagation · Modified extended tanh expansion method · Enhanced Riccati solutions

1 Introduction

Partial differential equations, especially NLSEs, can widely be used to model optical phenomena as used for phenomena in various areas. Generating the model for a physical event and obtaining exact, analytical or numerical solutions for the model are the main

✉ Mustafa Bayram
mustafabayram@biruni.edu.tr

Muslum Ozisik
ozisik@yildiz.edu.tr

Aydin Secer
asecer@yildiz.edu.tr

Melih Cinar
mcinar@yildiz.edu.tr

[1] Mathematical Engineering, Yildiz Technical University, Istanbul, Turkey

[2] Computer Engineering, Biruni University, Istanbul, Turkey

research subjects for many researchers. One of these models is optical modeling, which has come to the fore in recent years. There are some examples of optical modeling like optical image denoising (Qiao and Zou 2013), shock waves (Guner 2017), optical fiber pulses (Kudryashov 2020; Samir et al. 2021), light rays (Ren et al. 2019), electromagnetic analysis of dispersive media (Li et al. 2019), magneto-optic wave guides with different non-linearity (Ekici et al. 2017), thirring optical solitons (Bakodah et al. 2017), phase-shift controlling of solitons (Liu et al. 2019), 1-soliton solutions Biswas (2009), soliton transmission of optical fibers (Biswas and Arshed 2018).

Besides these models, with the help of computer-aided mathematical calculation programs, a wide variety of analytical and very efficient numerical methods have been developed in the recent years. For example, modified extended tanh method (Cinar et al. 2021), Sardar sub-equation method (Esen et al. 2021), extended rational sin-cos and sinh-cosh methods (Mahak and Akram 2019; Cinar et al. (2021; Mahak and Akram 2019; Cinar et al. 2021), Riccati Bernoulli sub-ODE method (Ozdemir et al. 2021), generated exponential function method (Srivastava et al. 2019), wavelet metods (Secer and Cinar 2020; Cinar et al. 2021), modified Kudryashov method (Srivastava et al. 2020) and the extended sinh-Gordon method (Dutta et al. 2020).Laplace-Adomian Decomposition (Gonzalez-Gaxiola 2022), the improved Adomian decomposition scheme (Al Qarni et al. 2022), Lie symmetry analysis (Bansal et al. 2018), analytic soliton solution (Liu et al. 2019), stationary soliton (Adem et al. 2021), sine-Gordon equation approach (Yildirim et al. 2021a, b), Modified Kudryashov's method (Biswas et al. 2018), improved modified extended tanh-function method (Mirzazadeh et al. 2017), extended trial equation and extended $\frac{G'}{G}$-expansion scheme (Ekici et al. 2016), unified Riccati equation, new mappig scheme (Zayed et al. 2021), semi-inverse variational principle (Zayed et al. 2021), the extended auxiliary equation approach and Jacobi's elliptic function method (Bansal et al. 2018); Yıldırım et al. 2022), the Kudryashov's integration scheme (Arnous et al. 2022; Ozisik et al. 2022).

In this work, we deal with the system of coupled NLSEs defined as Agrawal and Liao (1995); Baskonus et al. (2018).

$$\eta_1 u_{tt} + i\left(u_x + \eta_2 v_t\right) + \eta_3 |u|^2 u + \eta_4 v = 0, \tag{1}$$

$$\eta_1 v_{tt} + i\left(v_x + \eta_2 u_t\right) + \eta_3 |v|^2 v + \eta_4 u = 0, \tag{2}$$

where $i = \sqrt{-1}$, $u = u(x,t)$ and $v = v(x,t)$ are envelopes of the field, x is the co-ordinate of propagation, $\frac{1}{\eta_2}$ is the group-velocity mismatch, η_1 is the group-velocity dispersion, η_4 is the linear coupling coefficient and η_3 is defined as $\eta_3 = \frac{2\pi m_2}{kB_{eff}}$, where m_2 is the nonlinear refractive index, k is the wavelength and B_{eff} denotes effective mode area of each wavelength. To obtain the solution of the equation systems in this study, we used the computer algebra system as in previous studies (Guzel and Bayram 2006; Cinar et al. 2021; Akinlar et al. 2014).

Here, eMETEM has been applied to the dual-core optical equations in order to gain novel solutions. Some related researches on the method are the space-time fractional equal width and modified equal width equation (Raslan et al. 2017), modified Benjamin-Bona-Mahony and Zakharov-Kuznetsov equations (Taghizadeh and Mirzazadeh 2012).

The organization of the paper is as follows: Sect. 2 explains the algorithm of eMETEM (Ozisik et al. 2022). The application of the method to the dual-core optical fiber equations is added to the Sect. 3. The obtained results and illustrative figures are given in Sect. 4 and the conclusion of the study is included in the final section.

2 Method

Step 1: Consider the following NLPDE (Nonlinear Partial Differential Equation) and the traveling wave transformations, respectively:

$$F\left(\mathcal{M}, \frac{\partial \mathcal{M}}{\partial t}, \frac{\partial \mathcal{M}}{\partial x}, \frac{\partial^2 \mathcal{M}}{\partial t^2}, \frac{\partial^2 \mathcal{M}}{\partial x^2}, \frac{\partial^2 \mathcal{M}}{\partial x \partial t}, \dots\right) = 0, \tag{3}$$

$$\mathcal{M}(x,t) = e^{i\theta} M(\xi), \quad \theta = \beta_1 x - \beta_2 t, \quad \xi = p_1 x + p_2 t, \tag{4}$$

where β_1, β_2, p_1 and p_2 are real constants. Substituting Eq. (4) into Eq. (3), we obtain the following NLODE:

$$P\big(M(\xi), M'(\xi), M''(\xi), \dots\big) = 0, \tag{5}$$

where $'$ denotes the derivative of $M(\xi)$ with respect to ξ.

Step 2: Suppose that Eq. (5) admits the following equation as solution:

$$M(\xi) = A_0 + \sum_{i=1}^{m} A_i \kappa^i(\xi) + \sum_{i=1}^{m} B_i \kappa^{-i}(\xi), \tag{6}$$

where $A_0, A_1, \dots, A_m, B_1, \dots, B_m$ are real constants to be computed later (A_m and B_m should not be zero, simultaneously). We can find $m \in \mathbb{Z}^+$ by applying the balancing rule in Eq. (5). The $\kappa(\xi)$ satisfies the following Riccati differential equation:

$$\frac{d\kappa(\xi)}{d\xi} = \omega \mp [\kappa(\xi)]^2, \tag{7}$$

where ω is a real constant.

Step 3: Utilize the solutions of Eq. (7) are given in Table 1.

Step 4: Substituting Eq. (6) and its related derivatives into Eq. (5) and considering Eq. (7), one can get a polynomial in $\kappa(\xi)$. Gathering the coefficients of $\kappa(\xi)$ with the same power and equating each coefficient to zero, we get a system of algebraic equations.

Step 5: The unknowns $A_0, A_1, \dots, A_m, B_1, B_2, \dots, B_m, \beta_1, \beta_2, p_1, p_2$ and ω can be found by solving the set of algebraic equations in Step 4. Substituting the $\kappa_i(\xi)$ funtions given in the Table 1. into Eq. (6) and considering Eq. (4), the solutions of the NLPDE in Eq. (3) are found.

3 Application of the method

Let us consider Eq. (1) and the following wave transformations:

$$u(x,t) = e^{i\theta} U(\xi), \; v(x,t) = e^{i\theta} V(\xi), \; \xi = \delta x - \lambda t, \; \theta = \beta_1 x - \beta_2 t, \tag{8}$$

where δ, λ, β_1 and β_2 are non-zero real values. $\theta, \beta_1, \beta_2, \delta$ and λ stand for the phase component, the frequency, the wave number and the velocity of the wave, respectively.

Substituting the wave transformations in Eq. (8) into Eq. (1), we obtain the following equations from the real and the imaginary parts, respectively:

Table 1 The analytical solutions of Riccati Eq. (7)

$$\kappa_1^{\mp}(\xi) = \pm\sqrt{\pm\omega}\tanh\left(\sqrt{\pm\omega}(\xi+\xi_0)\right),$$
$$\kappa_2^{\mp}(\xi) = \pm\sqrt{\pm\omega}\coth\left(\sqrt{\pm\omega}(\xi+\xi_0)\right),$$
$$\kappa_3^{\mp}(\xi) = \pm\sqrt{\pm\omega}\left(\tanh\left(2\sqrt{\pm\omega}(\xi+\xi_0)\right) \mp i\lambda sech\left(2\sqrt{\pm\omega}(\xi+\xi_0)\right)\right),$$
$$\kappa_4^{\mp}(\xi) = \mp\frac{\left(w-\sqrt{\pm\omega}\tanh\left(\sqrt{\pm\omega}(\xi+\xi_0)\right)\right)}{\left(1\mp\sqrt{\pm\omega}\tanh\left(\sqrt{\pm\omega}(\xi+\xi_0)\right)\right)},$$
$$\kappa_5^{\mp}(\xi) = \mp\frac{\sqrt{\pm\omega}\left(5-4\cosh\left(2\sqrt{\pm\omega}(\xi+\xi_0)\right)\right)}{\left(3+4\sinh\left(2\sqrt{\pm\omega}(\xi+\xi_0)\right)\right)},$$
$$\kappa_6^{\mp}(\xi) = \mp\frac{\lambda\sqrt{\pm\omega(\alpha^2+\beta^2)}-\alpha\sqrt{\pm\omega}\cosh\left(2\sqrt{\pm\omega}(\xi+\xi_0)\right)}{\alpha\sinh\left(2\sqrt{\pm\omega}(\xi+\xi_0)\right)+\beta},$$
$$\kappa_7^{\mp}(\xi) = \lambda\sqrt{\pm\omega}\left[1-\frac{2\alpha}{\alpha+\cosh\left(2\sqrt{\pm\omega}(\xi+\xi_0)\right)\pm\lambda\sinh\left(2\sqrt{\pm\omega}(\xi+\xi_0)\right)}\right],$$
$$\kappa_8^{\mp}(\xi) = \mp\sqrt{\mp\omega}\tan\left(\sqrt{\mp\omega}(\xi+\xi_0)\right),$$
$$\kappa_9^{\mp}(\xi) = \pm\sqrt{\mp\omega}\cot\left(\sqrt{\mp\omega}(\xi+\xi_0)\right),$$
$$\kappa_{10}^{\mp}(\xi) = \mp\sqrt{\mp\omega}\left(\tan\left(2\sqrt{\mp\omega}(\xi+\xi_0)\right) \mp \sec\left(2\sqrt{\mp\omega}(\xi+\xi_0)\right)\right),$$
$$\kappa_{11}^{\mp}(\xi) = \pm\frac{\sqrt{\mp\omega}\left(1-\tan\left(\sqrt{\mp\omega}(\xi+\xi_0)\right)\right)}{\left(1+\tan\left(\sqrt{\mp\omega}(\xi+\xi_0)\right)\right)},$$
$$\kappa_{12}^{\mp}(\xi) = \mp\frac{\sqrt{\mp\omega}\left(4-5\cos\left(2\sqrt{\mp\omega}(\xi+\xi_0)\right)\right)}{\left(3+5\sin\left(2\sqrt{\mp\omega}(\xi+\xi_0)\right)\right)},$$
$$\kappa_{13}^{\mp}(\xi) = \mp\frac{\lambda\sqrt{\mp\omega(\alpha^2-\beta^2)}-\alpha\sqrt{\mp\omega}\cos\left(2\sqrt{\mp\omega}(\xi+\xi_0)\right)}{\alpha\sin\left(2\sqrt{\mp\omega}(\xi+\xi_0)\right)+\beta},$$
$$\kappa_{14}^{\mp}(\xi) = i\lambda\sqrt{\mp\omega}\left[1-\frac{2\alpha}{\alpha+\cos\left(2\sqrt{\mp\omega}(\xi+\xi_0)\right)\pm i\lambda\sin\left(2\sqrt{\mp\omega}(\xi+\xi_0)\right)}\right],$$
$$\kappa_{15}^{\mp}(\xi) = 1/(\xi+\xi_0),\ \omega=0,$$

where ξ_0 is a free real parameter and $\lambda = \mp 1$

$$\left(\beta_2\eta_2+\eta_4\right)V(\xi) - \left(\beta_2{}^2\eta_1+\beta_1\right)U(\xi) + \eta_3(U(\xi))^3 + \eta_1\lambda^2\frac{\mathrm{d}^2}{\mathrm{d}\xi^2}U(\xi) = 0, \tag{9}$$

$$\left(2\lambda\beta_2\eta_1+\delta\right)\frac{\mathrm{d}}{\mathrm{d}\xi}U(\xi) - \eta_2\lambda\frac{\mathrm{d}}{\mathrm{d}\xi}V(\xi) = 0. \tag{10}$$

Similarly, substituting Eq. (8) into Eq. (2), we obtain the following equations from the real and the imaginary parts, respectively:

$$\left(\beta_2\eta_2+\eta_4\right)U(\xi) - \left(\beta_2{}^2\eta_1+\beta_1\right)V(\xi) + \eta_3(V(\xi))^3 + \eta_1\lambda^2\frac{\mathrm{d}^2}{\mathrm{d}\xi^2}V(\xi) = 0, \tag{11}$$

$$\left(2\lambda\beta_2\eta_1 + \delta\right)\frac{\mathrm{d}}{\mathrm{d}\xi}V(\xi) - \eta_2\lambda\frac{\mathrm{d}}{\mathrm{d}\xi}U(\xi) = 0. \tag{12}$$

By considering the imaginary parts equations in eqs. (10) and (12), it can be seen that the system has a non-trivial solution $U(\xi) = V(\xi)$. So, from Eqs. (10) or (12), we get:

$$\lambda = -\frac{\delta}{2\beta_2\eta_1 - \eta_2}. \tag{13}$$

Taking Eqs. (9) or (11) into consideration, one can get:

$$\left(-\beta_2{}^2\eta_1 + \beta_2\eta_2 - \beta_1 + \eta_4\right)U(\xi) + \eta_3(U(\xi))^3 + \eta_1\lambda^2\frac{\mathrm{d}^2}{\mathrm{d}\xi^2}U(\xi) = 0. \tag{14}$$

Balancing the terms U'' and U^3 in Mahak and Akram (2019), we get $m = 1$. So, Eq. (6) turns into following form:

$$U(\xi) = A_0 + A_1\kappa(\xi) + B_1\frac{1}{\kappa(\xi)}, \tag{15}$$

where A_1 and B_1 should not be zero, simultaneously. Substituting the Eq. (15) and its necessary derivatives into Eq. (14), we get a polynomial form in $\kappa(\xi)$. Gathering the each term according to same power of $\kappa^i(\xi)$ and equating each coefficients to zero, we get the following system as:

$$\begin{aligned}
&\kappa^{-3}(\xi): \quad B_1\left(2\eta_3\left(\eta_1\beta_2 - (1/2)\eta_2\right)^2 B_1{}^2 + \delta^2\eta_1\omega^2\right) = 0,\\
&\kappa^{-2}(\xi): \quad \eta_3 A_0 B_1{}^2 = 0,\\
&\kappa^{-1}(\xi): \quad \left(\begin{array}{l} -2\beta_2{}^4\eta_1{}^3 + 4\beta_2{}^3\eta_1{}^2\eta_2\\ -2\eta_1\left(\left(\left(-3A_0{}^2 - 3A_1B_1\right)\eta_3 + \beta_1 - \eta_4\right)\eta_1 + (5/4)\eta_2{}^2\right)\beta_2{}^2\\ +2\left(\left(\left(-3A_0{}^2 - 3A_1B_1\right)\eta_3 + \beta_1 - \eta_4\right)\eta_1 + (1/4)\eta_2{}^2\right)\eta_2\beta_2\\ +\delta^2\eta_1 w - (1/2)\left(\left(-3A_0{}^2 - 3A_1B_1\right)\eta_3 + \beta_1 - \eta_4\right)\eta_2{}^2 \end{array}\right) B_1 = 0,\\
&\kappa^{0}(\xi): \quad A_0\left(-\eta_1\beta_2{}^2 + \eta_2\beta_2 + \left(A_0{}^2 + 6A_1B_1\right)\eta_3 + \eta_4 - \beta_1\right) = 0,\\
&\kappa^{1}(\xi): \quad \left(\begin{array}{l} -2\beta_2{}^4\eta_1{}^3 + 4\beta_2{}^3\eta_1{}^2\eta_2\\ -2\eta_1\left(\left(\left(-3A_0{}^2 - 3A_1B_1\right)\eta_3 + \beta_1 - \eta_4\right)\eta_1 + (5/4)\eta_2{}^2\right)\beta_2{}^2\\ +2\left(\left(\left(-3A_0{}^2 - 3A_1B_1\right)\eta_3 + \beta_1 - \eta_4\right)\eta_1 + (1/4)\eta_2{}^2\right)\eta_2\beta_2\\ +\delta^2\eta_1 w - (1/2)\left(\left(-3A_0{}^2 - 3A_1B_1\right)\eta_3 + \beta_1 - \eta_4\right)\eta_2{}^2 \end{array}\right) A_1 = 0,\\
&\kappa^{2}(\xi): \quad \eta_3 A_0 A_1{}^2 = 0,\\
&\kappa^{3}(\xi): \quad \left(2A_1{}^2\beta_2{}^2\eta_1{}^2\eta_3 + \left(-2A_1{}^2\beta_2\eta_2\eta_3 + \delta^2\right)\eta_1 + (1/2)A_1{}^2\eta_2{}^2\eta_3\right)A_1 = 0.
\end{aligned} \tag{16}$$

By solving this system, we get many solution sets. But we present some of the sets as follows:

$$DSet_1 = \left\{ \begin{array}{l} \omega = \frac{(\eta_1 \beta_2{}^2 - \eta_2 \beta_2 + \beta_1 - \eta_4)(2\eta_1 \beta_2 - \eta_2)^2}{8\delta^2 \eta_1}, A_0 = 0, \\ A_1 = \frac{\delta \sqrt{-2\eta_1 \eta_3}}{\eta_3 (2\eta_1 \beta_2 - \eta_2)}, B_1 = \frac{\sqrt{2}(\eta_1 \beta_2{}^2 - \eta_2 \beta_2 + \beta_1 - \eta_4)(2\eta_1 \beta_2 - \eta_2)}{8\delta \sqrt{-\eta_1 \eta_3}} \end{array} \right\},$$

$$DSet_2 = \left\{ \begin{array}{l} \beta_1 = \frac{-4\beta_2{}^4 \eta_1{}^3 + (8\beta_2{}^3 \eta_2 + 4\beta_2{}^2 \eta_4)\eta_1{}^2 + \Omega_0 \eta_1 + \eta_2{}^2 (\eta_2 \beta_2 + \eta_4)}{(2\eta_1 \beta_2 - \eta_2)^2}, \\ A_0 = 0, A_1 = \frac{\delta \sqrt{-2\eta_1 \eta_3}}{\eta_3 (2\eta_1 \beta_2 - \eta_2)}, B_1 = \frac{w\delta \sqrt{-2\eta_1 \eta_3}}{\eta_3 (2\eta_1 \beta_2 - \eta_2)} \end{array} \right\},$$

$$DSet_3 = \left\{ \begin{array}{l} A_0 = 0, A_1 = \frac{16 w \eta_1{}^2 \delta^2}{\sqrt{\eta_1 \eta_3 (\Omega_2 - \Omega_3) w (\Omega_4 - \Omega_3)}}, \beta_2 = \frac{2\eta_2 + \sqrt{2\Omega_4 - 2\Omega_3}}{4\eta_1}, \\ B_1 = -\frac{\sqrt{\eta_1 \eta_3 (\Omega_2 - \Omega_3) w}}{4\eta_1 \eta_3} \end{array} \right\},$$

$$DSet_4 = \left\{ \begin{array}{l} A_0 = 0, A_1 = \frac{16\delta^2 \eta_1{}^2 w}{\sqrt{\eta_1 \eta_3 w (\Omega_2 + \Omega_3)(\Omega_3 + \Omega_4)}}, \beta_2 = \frac{\sqrt{2\Omega_3 + 2\Omega_4} + 2\eta_2}{4\eta_1}, \\ B_1 = -\frac{\sqrt{\eta_1 \eta_3 w (\Omega_2 + \Omega_3)}}{4\eta_1 \eta_3} \end{array} \right\},$$

where

$$\begin{aligned} \Omega_0 &= \left(-5\beta_2{}^2 \eta_2{}^2 - 4\delta^2 w - 4\beta_2 \eta_2 \eta_4\right), \\ \Omega_1 &= \left(-64\delta^2 w + 16\beta_1^2 - 32\beta_1 \eta_4 + 16\eta_4^2\right)\eta_1^2, \Omega_2 = 4\beta_1 \eta_1 - 4\eta_4 \eta_1 - \eta_2^2, \\ \Omega_3 &= \sqrt{\Omega_1 + 8\eta_2^2 (\eta_4 - \beta_1)\eta_1 + \eta_2^4}, \Omega_4 = (4\eta_4 - 4\beta_1)\eta_1 + \eta_2^2, \end{aligned} \tag{17}$$

Substituting the $\kappa_j(\xi)$ in Table 1 into Eq. (15) and using the Eq. (8), the following solution functions $u_j(x,t) = v_j(x,t)$ for the NLSE system in eqs. (1) and (2) are obtained in the general form for $j = 1, 2, \ldots, 15$:

$$u_1(\mathrm{x,t}) = \chi\left(A_0 - A_1 \sqrt{-\omega} \tanh\left(P_{\omega xt}\right) - \frac{B_1}{\sqrt{-\omega} \tanh\left(P_{\omega xt}\right)} \right), \tag{18}$$

$$u_2(\mathrm{x,t}) = \chi\left(A_0 - A_1 \sqrt{-\omega} \coth\left(P_{\omega xt}\right) - \frac{B_1}{\sqrt{-\omega} \coth\left(P_{\omega xt}\right)} \right), \tag{19}$$

$$u_3(\mathrm{x,t}) = \chi\left(\begin{array}{l} A_0 - A_1 \sqrt{-\omega}\left(\tanh\left(2P_{\omega xt}\right) + i\mu \operatorname{sech}\left(2P_{\omega xt}\right)\right) \\ -\frac{B_1}{\sqrt{-\omega}\left(\tanh\left(2P_{\omega xt}\right) + i\mu \operatorname{sech}\left(2P_{\omega xt}\right)\right)} \end{array} \right), \tag{20}$$

$$u_4(\mathrm{x,t}) = \chi\left(A_0 + A_1 \frac{\omega - \sqrt{-\omega} \tanh\left(P_{\omega xt}\right)}{1 + \sqrt{-\omega} \tanh\left(P_{\omega xt}\right)} + B_1 \frac{1 + \sqrt{-\omega} \tanh\left(P_{\omega xt}\right)}{\omega - \sqrt{-\omega} \tanh\left(P_{\omega xt}\right)} \right), \tag{21}$$

$$u_5(\mathrm{x,t}) = \chi\left(A_0 + A_1 \frac{\sqrt{-\omega}\left(5 - 4\cosh\left(2P_{\omega xt}\right)\right)}{3 + 4\sinh\left(2P_{\omega xt}\right)} + B_1 \frac{3 + 4\sinh\left(2P_{\omega xt}\right)}{\sqrt{-\omega}\left(5 - 4\cosh\left(2P_{\omega xt}\right)\right)} \right), \tag{22}$$

$$u_6(\mathrm{x,t}) = \chi\left(\begin{array}{l} A_0 + A_1 \frac{\mu\sqrt{-(a^2+b^2)\omega}-a\sqrt{-\omega}\cosh\left(2P_{\omega xt}\right)}{a\sinh\left(2\sqrt{-\omega}\eta(x-vt)\right)+b} \\ +B_1 \frac{a\sinh\left(2P_{\omega xt}\right)+b}{\mu\sqrt{-(a^2+b^2)\omega}-a\sqrt{-\omega}\cosh\left(2P_{\omega xt}\right)} \end{array}\right), \tag{23}$$

$$u_7(\mathrm{x,t}) = \chi\left(\begin{array}{l} A_0 + A_1\left(\mu\sqrt{-\omega} - 2\frac{\mu a\sqrt{-\omega}}{a+\cosh\left(2P_{\omega xt}\right)-\mu\sinh\left(2P_{\omega xt}\right)}\right) \\ +\frac{B_1}{\mu\sqrt{-\omega}-2\frac{\mu a\sqrt{-\omega}}{a+\cosh\left(2P_{\omega xt}\right)-\mu\sinh\left(2P_{\omega xt}\right)}} \end{array}\right), \tag{24}$$

$$u_8(\mathrm{x,t}) = \chi\left(A_0 + A_1\sqrt{\omega}\tan\left(Q_{\omega xt}\right) + \frac{B_1}{\sqrt{\omega}\tan\left(Q_{\omega xt}\right)}\right), \tag{25}$$

$$u_9(\mathrm{x,t}) = \chi\left(A_0 - A_1\sqrt{\omega}\cot\left(Q_{\omega xt}\right) - \frac{B_1}{\sqrt{\omega}\cot\left(Q_{\omega xt}\right)}\right), \tag{26}$$

$$u_{10}(\mathrm{x,t}) = \chi\left(A_0 + A_1\sqrt{\omega}\left(\tan\left(2Q_{\omega xt}\right) + \mu\sec\left(2Q_{\omega xt}\right)\right) + \frac{B_1}{G_0}\right), \tag{27}$$

where $G_0 = \sqrt{\omega}\tan\left(2Q_{\omega xt}\right) + \mu\sec\left(2Q_{\omega xt}\right)$.

$$u_{11}(\mathrm{x,t}) = \chi\left(A_0 - A_1\frac{\sqrt{\omega}\left(1-\tan\left(Q_{\omega xt}\right)\right)}{1+\tan\left(Q_{\omega xt}\right)} - B_1\frac{1+\tan\left(Q_{\omega xt}\right)}{\sqrt{\omega}\left(1-\tan\left(Q_{\omega xt}\right)\right)}\right), \tag{28}$$

$$u_{12}(\mathrm{x,t}) = \chi\left(A_0 + A_1\frac{\sqrt{\omega}\left(4-5\cos\left(2Q_{\omega xt}\right)\right)}{3+5\sin\left(2Q_{\omega xt}\right)} + B_1\frac{3+5\sin\left(2Q_{\omega xt}\right)}{\sqrt{\omega}\left(4-5\cos\left(2Q_{\omega xt}\right)\right)}\right), \tag{29}$$

$$u_{13}(\mathrm{x,t}) = \chi\left(A_0 + A_1\frac{\mu G_1}{a\sin\left(2Q_{\omega xt}\right)+b} + B_1\frac{a\sin\left(2Q_{\omega xt}\right)+b}{\mu\sqrt{\left(a^2-b^2\right)\omega} - a\sqrt{\omega}\cos\left(2Q_{\omega xt}\right)}\right), \tag{30}$$

where $G_1 = \sqrt{\left(a^2-b^2\right)\omega} - a\sqrt{\omega}\cos\left(2Q_{\omega xt}\right)$.

$$u_{14}(\mathrm{x,t}) = \chi\left(\begin{array}{l} A_0 + A_1\left(i\mu\sqrt{\omega} - \frac{2i\mu a\sqrt{\omega}}{a+\cos\left(2Q_{\omega xt}\right)-i\mu\sin\left(2Q_{\omega xt}\right)}\right) \\ +\frac{B_1}{\left(i\mu\sqrt{\omega}-\frac{2i\mu a\sqrt{\omega}}{a+\cos\left(2Q_{\omega xt}\right)-i\mu\sin\left(2Q_{\omega xt}\right)}\right)} \end{array}\right), \tag{31}$$

$$u_{15}(\mathrm{x,t}) = -\frac{1}{\delta x - \lambda t}, \tag{32}$$

where $\chi = e^{i(-t\beta_2 + x\beta_1)}$, $\lambda = \frac{\delta}{\eta_2 - 2\eta_1\beta_2}$, $P_{\omega xt} = \sqrt{-\omega}(\delta x - \lambda t)$, $Q_{\omega xt} = \sqrt{\omega}(\delta x - \lambda t)$ and $v_j(\mathrm{x,t}) = u_j(\mathrm{x,t}), (\mathrm{j} = 1, 2, \dots, 15)$.

4 Results and discussion

In this section, we have presented various graphical illustrations of selected some of the solution functions obtained in the study. In Fig. 1, we give the some graphical illustrations of $u_3(x,t)$ in Eq. (20) for the parameters $\eta_1 = -0.25, \eta_2 = 0.3, \eta_3 = 0.75, \eta_4 = 0.15, \beta_1 = 0.85, \beta_2 = 1.25, \delta = 2$ and $\mu = 1$ with $DSet_1$. The Fig. 1a–c give the representation of anti-peaked soliton. The Fig. 1c also reflects traveling wave property. The Fig. 1d–f belong to the imaginary part of $u_3(x,t)$, and a periodic bright-dark soliton with different amplitudes is formed for the investigated case.

In Fig. 2, the some plots of $u_3(x,t)$ in Eq. (20) are demonstrated for the parameters $\omega = -0.4, \eta_1 = 0.65, \eta_2 = 0.15, \eta_3 = 0.25, \eta_4 = 0.5, \beta_2 = 0.6, \delta = 0.85$ and $\mu = 1$ with $DSet_2$. The Fig. 2a–c represents a bright soliton. The Fig. 2c also reflects the traveling wave feature. The Fig. 2d–f belong to the imaginary part of $u_3(x,t)$, producing a lump-shaped soliton for the case under consideration.

In Fig. 3, the some views of $u_6(x,t)$ in Eq. (23) are illustrated for the parameters $\omega = -0.4, \eta = 1, \eta_1 = 1.65, \eta_2 = 1.55, \eta_3 = 2.25, \eta_4 = 2.5, \beta_1 = 0.25, \delta = 0.2$ and $\mu = 1$ with $DSet_3$. When the Fig. 3a–c are viewed from the x-axis direction, they demonstrate a bright soliton without traveling wave feature. The Fig. 3d–f belong to the imaginary part of $u_6(x,t)$, and a degenerate dark-bright-like image is formed for the examined situation.

In Fig. 4, we present some portraits of $u_{14}(x,t)$ in Eq. (31) by selecting the parameters $\omega = 0.04, \eta_1 = 0.65, \eta_2 = 0.15, \eta_3 = 0.25, \eta_4 = 0.5, \beta_2 = 0.6, \delta = 0.85$, $a = 1.2$, $b = 0.6$ and $\mu = 1$ with $DSet_2$. The Fig. 4a–c have a periodic bright soliton behavior. The Fig. 4c shows the traveling wave feature. The Fig. 4d–f belong to the imaginary part of $u_{14}(x,t)$ and produce a rogue wave style soliton for the case under consideration.

In Fig. 5, the some silhouettes of $u_{14}(x,t)$ in Eq. (31) are given for the parameters $\omega = 0.00004, \eta_1 = 0.65, \eta_2 = 0.15, \eta_3 = 0.25, \eta_4 = 0.5, \beta_2 = 0.6, \delta = 0.85$, $a = 1.2$, $b = 0.6$ and $\mu = 1$ with $DSet_2$. The Fig. 5a–c illustrate a compacton-style soliton without a traveling wave image. In a sense, it can also be called a parabolic soliton. The Fig. 5d–f belong to the imaginary part of $u_{14}(x,t)$, producing periodic bright-dark solitons of variable amplitude.

In Fig. 6, the some depictions of $u_{14}(x,t)$ in Eq. (31) are presented for the parameters $\omega = 0.4, \eta_1 = 1.65, \eta_2 = 1.55, \eta_3 = 2.25, \eta_4 = 2.5, \beta_1 = 0.25, \delta = 0.2$, $a = 1.2$, $b = 0.6$ and $\mu = 1$ with $DSet_4$. The Fig. 6a–c represent a periodic bright soliton. The Fig. 6d–f belong to the imaginary part of $u_{14}(x,t)$ and show variable types of degenerate lump-like soliton.

In Fig. 7, we investigate the effect of the group velocity dispersion on the $u_3(x,t)$ in Eq. (20) for the parameters $\eta_2 = 0.3, \eta_3 = 0.75, \beta_1 = 0.85, \beta_2 = 1.25, \delta = 2$ and $\mu = 1$ with $DSet_1$. In Fig. 7a, taking $\eta_4 = -0.15$ and choosing $\eta_1 < 0$, the chromatic dispersion term coefficient η_1 are selected as $-0.0025, -0.050, -0.075, -0.100, -0.125, -0.150, -0.175, -0.200, -0.225 and -0.250$, respectively. When the obtained figures are examined, if $\eta_1 < 0$ and η_1 increase, the lower peak of the wave remains on the horizontal x-axis, but the soliton moves to the right. At the same time, there is an increase in the vertical amplitude of the soliton.

In Fig. 7b the same examination is made for $\eta_1 > 0$ and $\eta_4 = 0.95$, the lower peak of the soliton stays on the horizontal axis due to the increase in $\eta_1 > 0$ and η_1, and the peak moves horizontally depending on the changing η_1 values. However, this movement is not just a

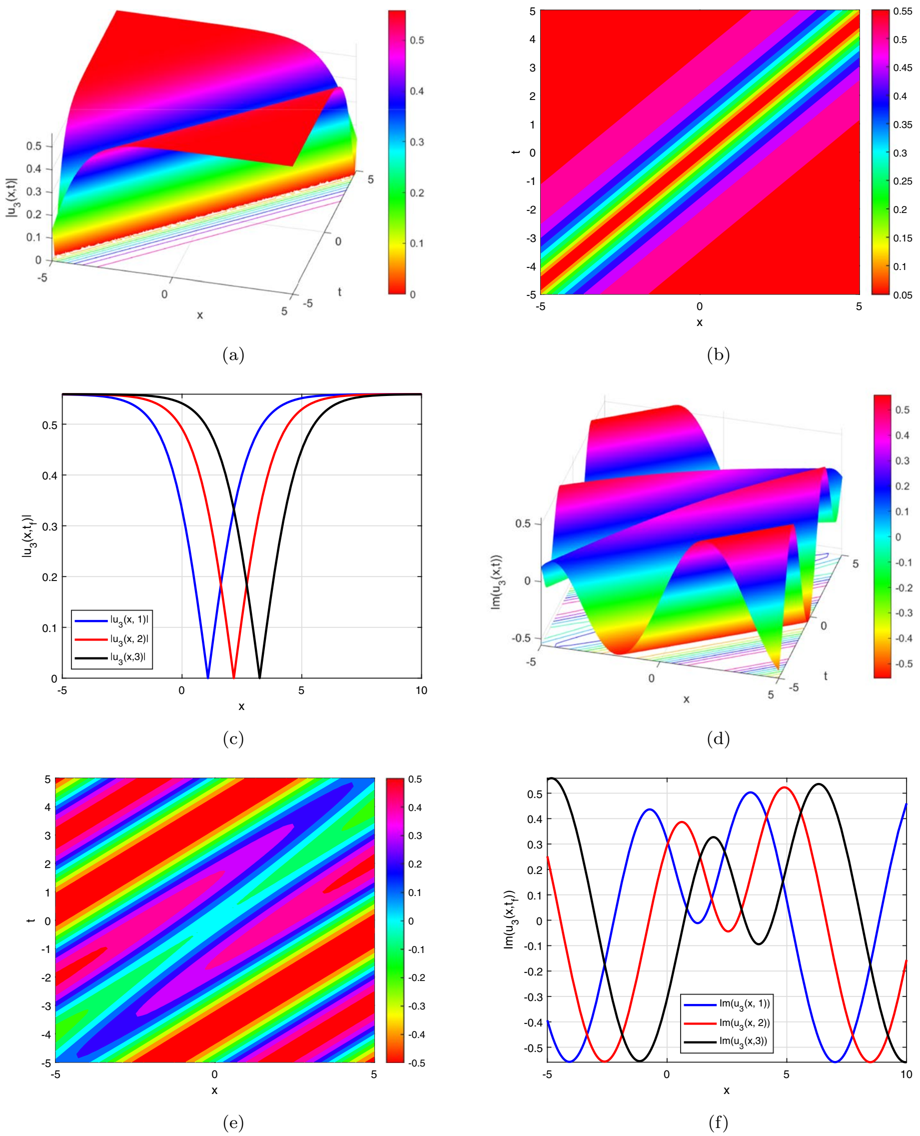

Fig. 1 The some graphical illustrations of $u_3(x, t)$ given in Eq. (20) **a** 3D view of $|u_3(x, t)|$, **b** the contour view of $|u_3(x, t)|$, **c** 2D view of $|u_3(x, t)|$, **d** 3D view of $Im\big(u_3(x, t)\big)$, **e** the contour of $Im\big(u_3(x, t)\big)$, **f** the 2D view of $Im\big(u_3(x, t)\big)$

movement to the right or the left, as we obtained in our previous examination, the movement varies. The reason for this variability can be explained by the difficulty in controlling chromatic dispersion in optical wave propagation. Moreover, the increase in η_1 values causes a decrease in the vertical amplitude of the soliton and also affects the shape of the soliton. For example, when $\eta_1 = 0.135$, the soliton often refers to a V-type soliton.

In Fig. 8, the effect of the chromatic dispersion on the $u_3(x, t)$ in Eq. (20) is investigated for the parameters $\omega = -0.4, \eta_2 = 0.15, \eta_3 = 0.25, \eta_4 = 0.95, \beta_2 = 0.6, \delta = 0.85$

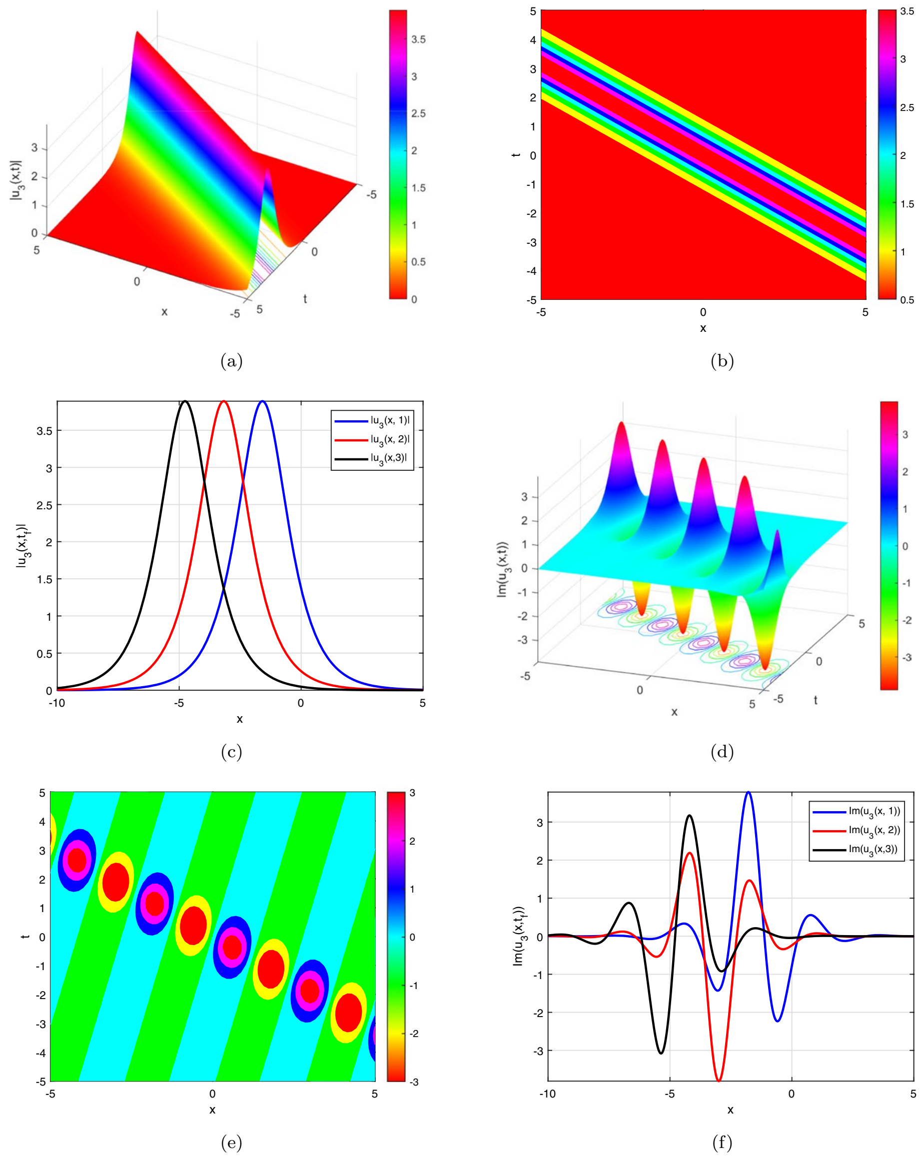

Fig. 2 The some graphical illustrations of $u_3(x,t)$ given in Eq. (20) **a** 3D view of $|u_3(x,t)|$, **b** the contour view of $|u_3(x,t)|$, **c** 2D view of $|u_3(x,t)|$, **d**3D view of $Im\big(u_3(x,t)\big)$, **d** the contour of $Im\big(u_3(x,t)\big)$, **d** the 2D view of $Im\big(u_3(x,t)\big)$

and $\mu = 1$ with $DSet_2$. In Fig. 8a, an examination is made for $\eta_1 < 0$. As a result of the examination, when $\eta_1 < 0$ and η_1 increase, the soliton maintains its general shape in terms of species, that is, the bright soliton character continues, the skirts of the soliton remain on the horizontal axis, but the soliton moves to the right. At the same time, there is a change in the vertical amplitude of the soliton. It is not possible to characterize this

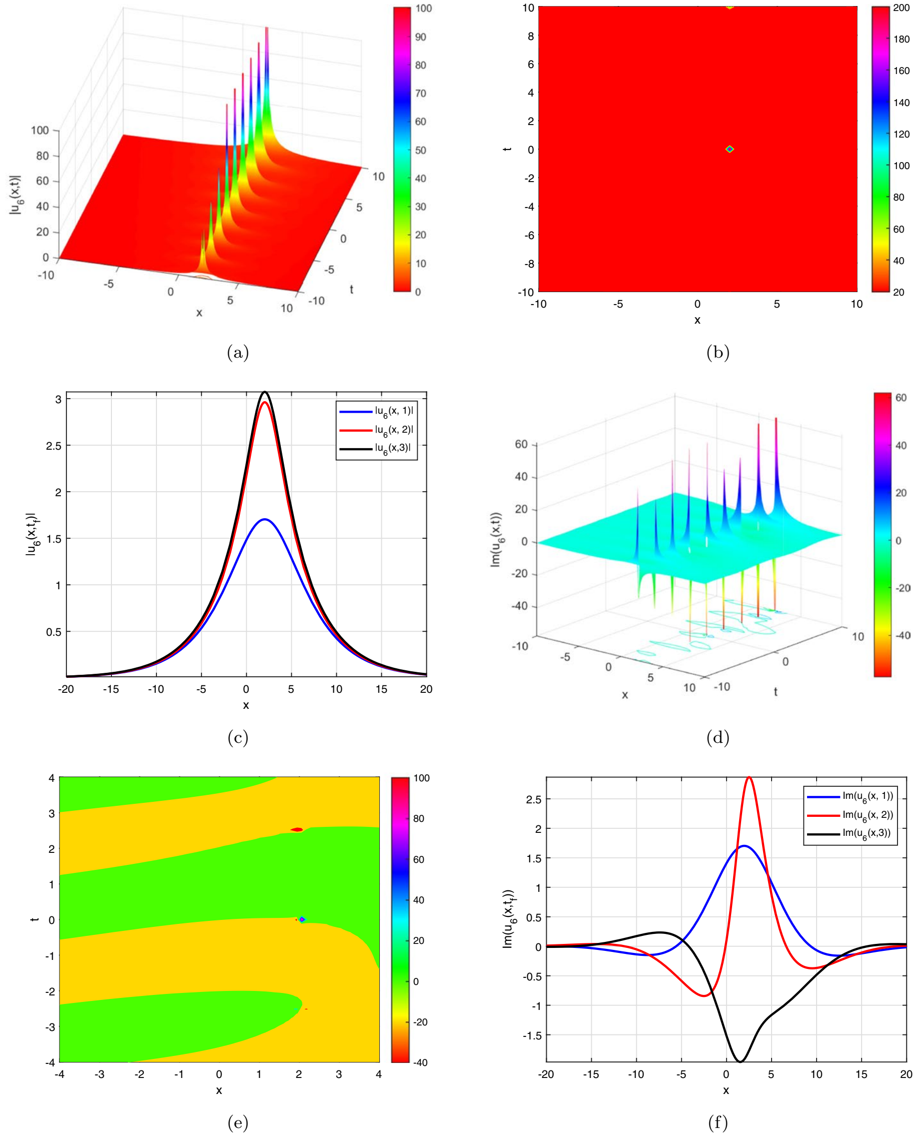

Fig. 3 The some views of $u_6(x,t)$ given in Eq. (23) **a** 3D view of $|u_6(x,t)|$, **b** the contour view of $|u_6(x,t)|$, **c** 2D view of $|u_6(x,t)|$, **d** 3D view of $Im\big(u_6(x,t)\big)$, **e** the contour of $Im\big(u_6(x,t)\big)$, **f** the 2D view of $Im\big(u_6(x,t)\big)$

change as a regular increase or decrease. As can be seen from the Fig. 8a, there is an increase for some values and a decrease for some values.

In Fig. 8b, while $\eta_1 > 0$ and η_1 increase, an examination is made. As a result of the examination, the soliton still maintains its bright soliton feature, and the skirts of the soliton remain on the x-axis. However, there are dramatic changes in the position and amplitude of the soliton. When the Fig. 8b is examined in detail, it is observed that the change in the position and amplitude (pulse beats) of the soliton is random. The

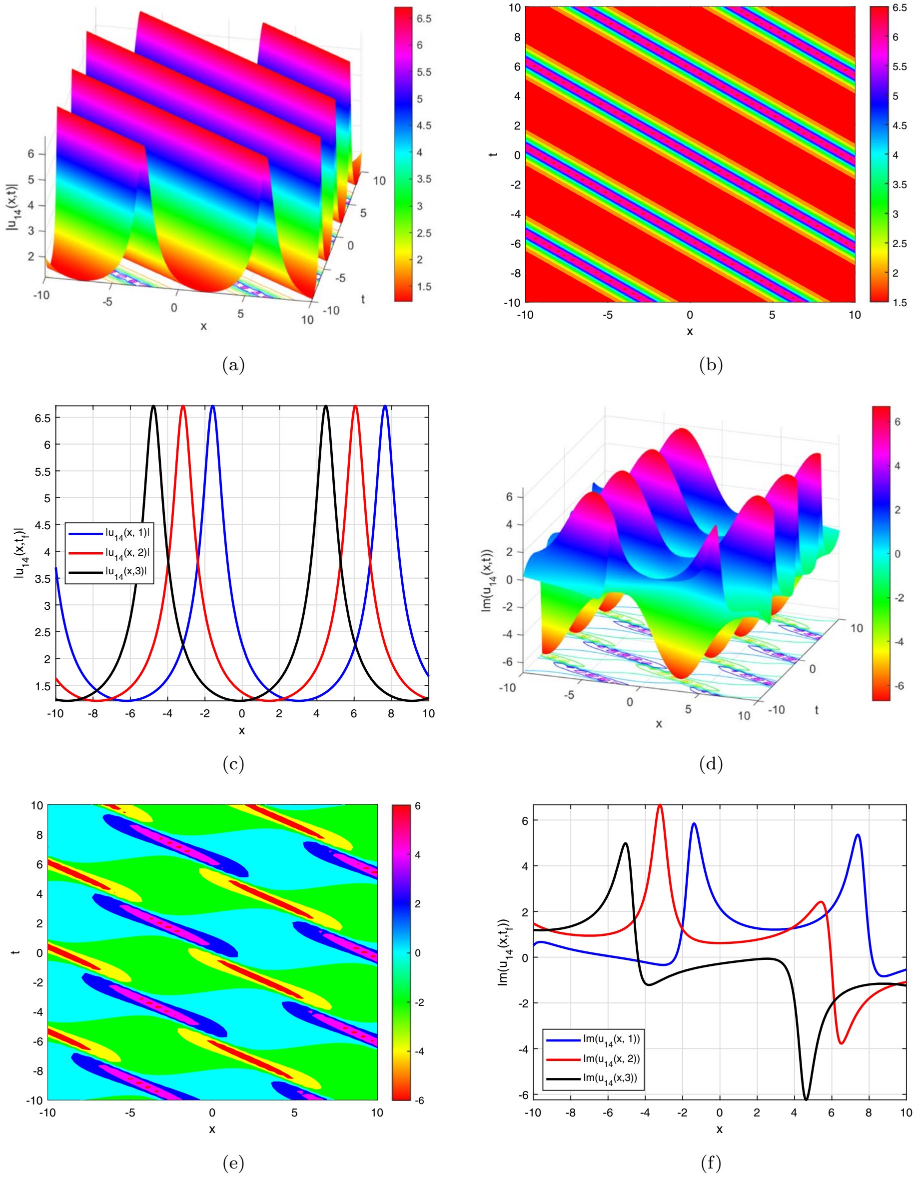

Fig. 4 The some portraits of $u_{14}(x,t)$ given in Eq. (31) **a** 3D view of $|u_{14}(x,t)|$, **b** the contour view of $|u_{14}(x,t)|$, **c** 2D view of $|u_{14}(x,t)|$, **d** 3D view of $Im\big(u_{14}(x,t)\big)$, **e** the contour of $Im\big(u_{14}(x,t)\big)$, **f** the 2D view of $Im\big(u_{14}(x,t)\big)$

randomness can also be explained as the difficulty in controlling the GVD. For example, although $\eta_1 = -0.125$ in Fig. 8a, it is chosen as 0.135 instead of 0.125 in Fig. 8b. Moreover, in this case, the η_4 value is taken as 0.95 instead of 0.15. The reason for this is that if $\eta_1 = 0.125, \eta_4 = 0.15$ are taken, the soliton turns into a completely different shape. Thus, in a sense, the GVD is controlled by the nonlinear term within the

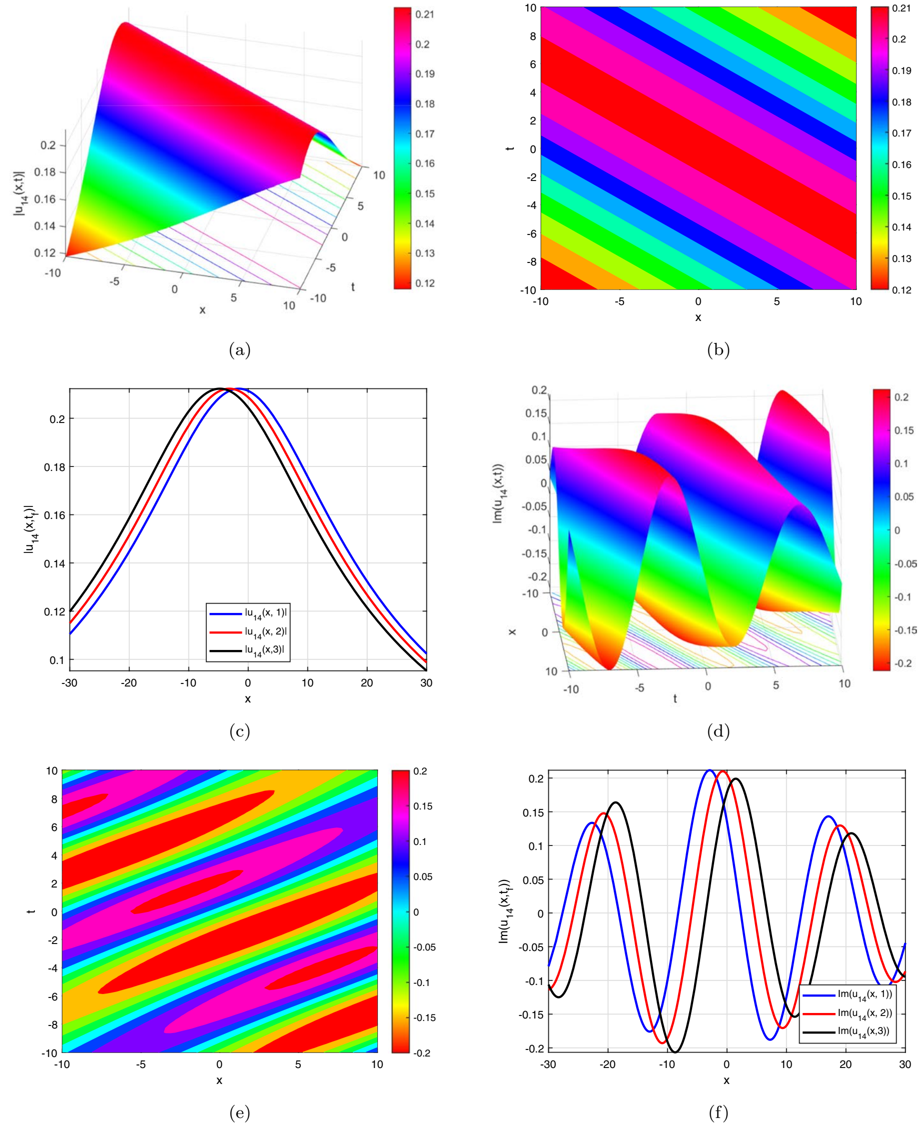

Fig. 5 The some silhouettes of $u_{14}(x,t)$ given in Eq. (31) **a** 3D view of $|u_{14}(x,t)|$, **b** the contour view of $|u_{14}(x,t)|$, **c** 2D view of $|u_{14}(x,t)|$, **d** 3D view of $Im\big(u_{14}(x,t)\big)$, **e** the contour of $Im\big(u_{14}(x,t)\big)$, **f** the 2D view of $Im\big(u_{14}(x,t)\big)$

perturbation term. This situation alone shows how difficult it is to control the terms group velocity dispersion, chromatic dispersion, and inter-modal dispersion in optical fibers. Therefore, studies on these situations are important and a great need.

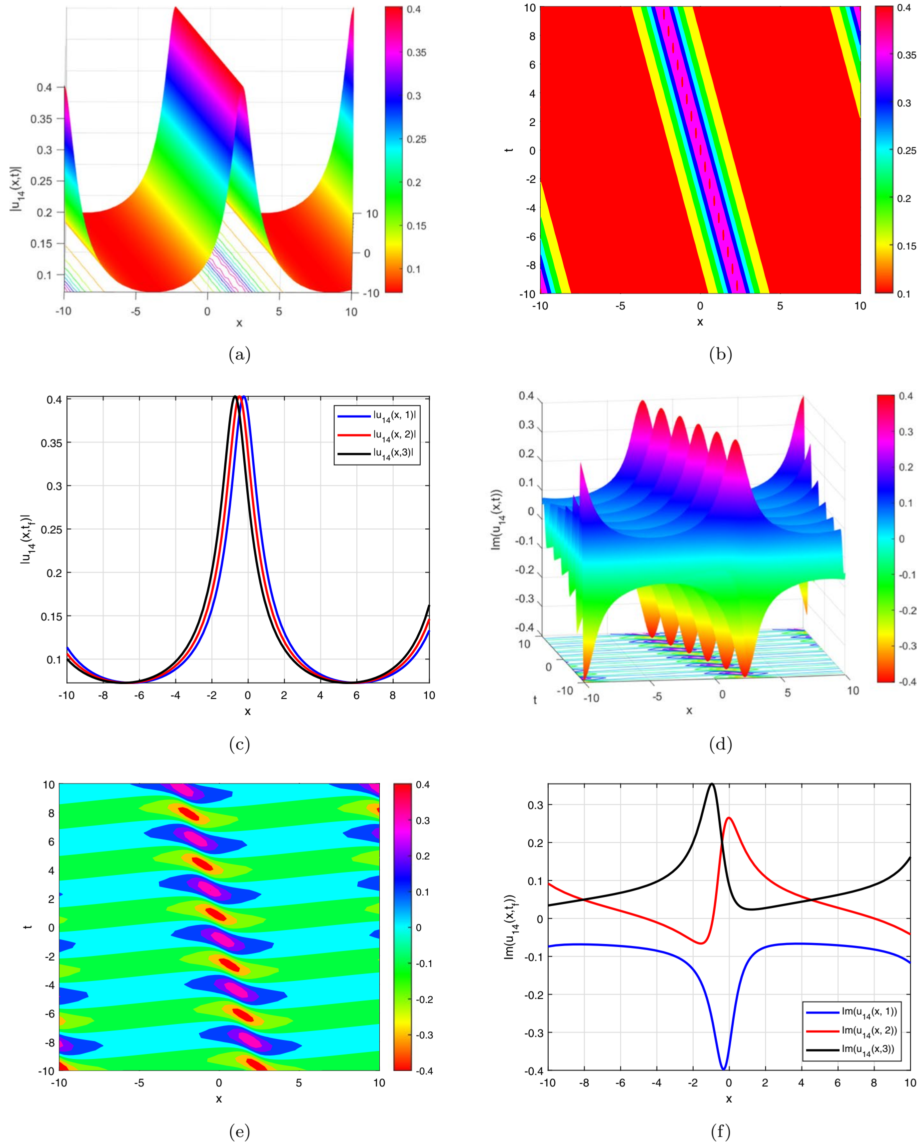

Fig. 6 The some depictions of $u_{14}(x,t)$ given in Eq. (31) **a** 3D view of $|u_{14}(x,t)|$, **b** the contour view of $|u_{14}(x,t)|$, **c** 2D view of $|u_{14}(x,t)|$, **d** 3D view of $Im\big(u_{14}(x,t)\big)$, **e** the contour of $Im\big(u_{14}(x,t)\big)$, **f** the 2D view of $Im\big(u_{14}(x,t)\big)$

5 Conclusion

In this study, the nonlinear Schrödinger equation, which has an important place in modeling soliton transmission in optical fibers, has been discussed and successfully investigated. As a result of the examination, many soliton solutions and graphics have been obtained and interpreted in detail, and the comments made with 3D, contour and 2D

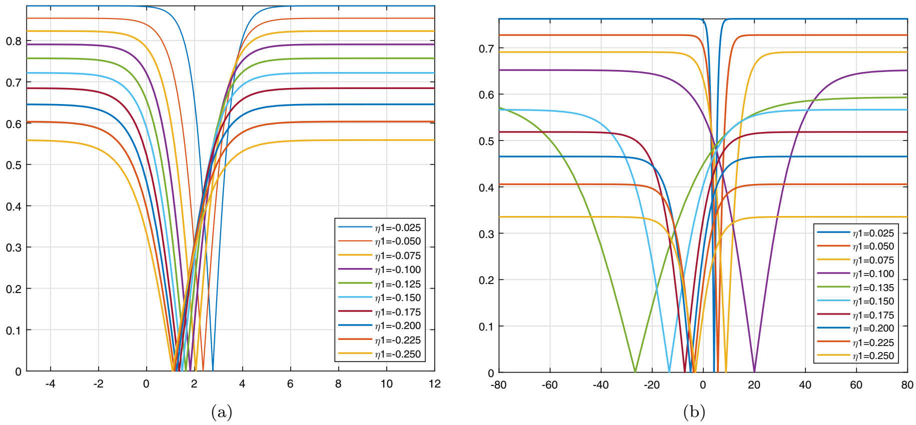

Fig. 7 The effect of the coefficient of the GVD on the $u_3(x,t)$ in Eq. (20) by selected parameters $\eta_2 = 0.3, \eta_3 = 0.75, \beta_1 = 0.85, \beta_2 = 1.25, \delta = 2$ and $\mu = 1$ with $DSet_1$ **a** $\eta_1 < 0$ and $\eta_4 = -0.15$, **b** $\eta_1 > 0$ and $\eta_4 = 0.95$

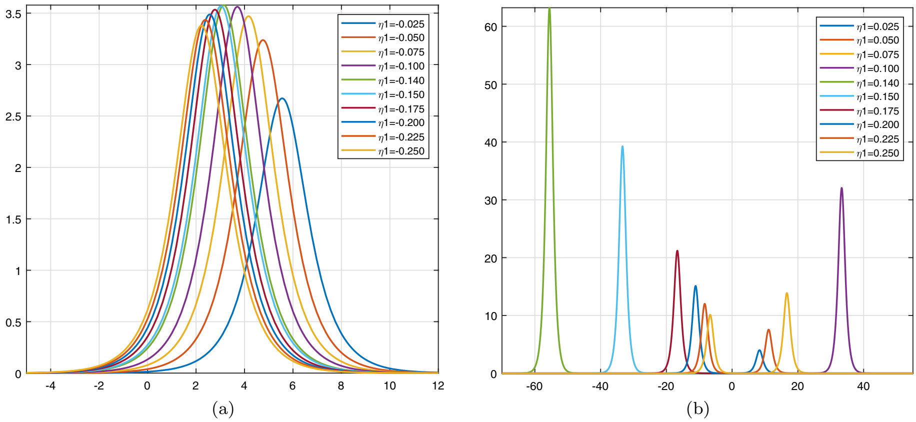

Fig. 8 The effect of the coefficient of the GVD on the $u_3(x,t)$ in Eq. (20) by selected parameters $\omega = -0.4, \eta_2 = 0.15, \eta_3 = 0.25, \eta_4 = 0.95, \beta_2 = 0.6, \delta = 0.85$ and $\mu = 1$ with $DSet_2$ **a** $\eta_1 < 0$, **b** $\eta_1 > 0$

graphics have been demonstrated. The study is not only about obtaining the soliton solutions of the NLSE equation, but also the eMETEM method has been successfully applied. As a more important contribution of this paper, the effect of the coefficient of the GVD dispersion term on the soliton propagation has been investigated. Considering the effect of the term coefficient of the GVD dispersion on soliton transmission in optical fibers and the difficulty in controlling this effect, the obtained results in the study might contribute to future studies in this field.

Author contributions All parts contained in the research carried out by the authors through hard work and a review of the various references and contributions in the field of mathematics and Applied physics.

Funding No funding for this article.

Availability of data and materials Data sharing is not applicable to this article as no datasets were generated or analyzed during the current study.

Declarations

Conflict of interest This research received no specific grant from any funding agency in the public, commercial or not-for-profit sectors. The authors did not have any competing interests in this research.

Ethical approval The Corresponding Author, declare that this manuscript is original, has not been published before, and is not currently being considered for publication elsewhere. The Corresponding Author confirm that the manuscript has been read and approved by all the named authors and there are no other persons who satisfied the criteria for authorship but are not listed. I further confirm that the order of authors listed in the manuscript has been approved by all of us. we understand that the Corresponding Author is the sole contact for the Editorial process and is responsible for communicating with the other authors about progress, submissions of revisions, and final approval of proofs.

References

Adem, A., Ntsime, B., Biswas, A., Khan, S., Alzahrani, A., Belić, M.: Stationary optical solitons with nonlinear chromatic dispersion for Lakshmanan-Porsezian-Daniel model having Kerr law of nonlinear refractive index. Ukr. J. Phys. Opt. **22**, 83–86 (2021). https://doi.org/10.3116/16091833/22/2/83/2021

Agrawal, G., Liao, P.: Nonlinear Fiber Optics. Academic Press, Cambridge (1995)

Akinlar, M.A., Secer, A., Bayram, M.: Numerical solution of fractional benney equation, Appl. Math. Inf. Sci. **8**(4), 1633–1637 (2014) https://doi.org/10.12785/amis/080418

Al-Qarni, A.A., Bodaqah, A.M., Mohammed, A.S.H.F., Alshaery, A.A., Bakodah, H.O., Biswas, A.: Cubic-quartic optical solitons for Lakshmanan-Porsezian-Daniel equation by the improved adomian decomposition scheme. Ukr. J. Phys. Opt. **23**(4), 228–242 (2022). https://doi.org/10.3116/16091833/23/4/XXXXX/2022

Arnous, A.H., Nofal, T.A., Biswas, A., Khan, S., Moraru, L.: Quiescent optical solitons with Kudryashov's generalized quintuple-power and nonlocal nonlinearity having nonlinear chromatic dispersion. Universe **8**(10), 501 (2022). https://doi.org/10.3390/universe8100501

Bakodah, H.O., Al-Qarni, A.A., Banaja, M.A., Zhou, Q., Moshokoa, S.P., Biswas, A.: Bright and dark Thirring optical solitons with improved adomian decomposition method. Optik **130**, 1115–1123 (2017). https://doi.org/10.1016/J.IJLEO.2016.11.123

Bansal, A., Biswas, A., Zhou, Q., Babatin, M.: Lie symmetry analysis for cubic-quartic nonlinear schrödinger's equation. Optik **169**, 12–15 (2018). https://doi.org/10.1016/j.ijleo.2018.05.030

Baskonus, H.M., Sulaiman, T.A., Bulut, H.: Dark, bright and other optical solitons to the decoupled nonlinear Schrödinger equation arising in dual-core optical fibers. Opt. Quantum Electron. **50**(4), 1–12 (2018). https://doi.org/10.1007/s11082-018-1433-0

Biswas, A.: 1-soliton solution of the generalized Radhakrishnan, Kundu, Lakshmanan. Equ. Phys. Lett. A **373**(30), 2546–2548 (2009). https://doi.org/10.1016/J.PHYSLETA.2009.05.010

Biswas, A., Arshed, S.: Optical solitons in presence of higher order dispersions and absence of self-phase modulation. Optik **174**, 452–459 (2018). https://doi.org/10.1016/J.IJLEO.2018.08.037

Biswas, A., Rezazadeh, H., Mirzazadeh, M., Eslami, M., Ekici, M., Zhou, Q., Moshokoa, S.P., Belic, M.: Optical soliton perturbation with fokas-lenells equation using three exotic and efficient integration schemes. Optik **165**, 288–294 (2018). https://doi.org/10.1016/j.ijleo.2018.03.132

Cinar, M., Onder, I., Secer, A., Sulaiman, T.A., Yusuf, A., Bayram, M.: Optical solitons of the (2+1)-dimensional Biswas-Milovic equation using modified extended tanh-function method. Optik **245**, 167631 (2021). https://doi.org/10.1016/J.IJLEO.2021.167631

Cinar, M., Onder, I., Secer, A., Yusuf, A., Sulaiman, T.A., Bayram, M., Aydin, H.: Soliton Solutions of (2+1) Dimensional Heisenberg Ferromagnetic Spin Equation by the Extended Rational sine-cosine and sinh-cosh Method. Int. J. Appl. Comput. Math. **7**(4), 1–17 (2021). https://doi.org/10.1007/s40819-021-01076-5

Cinar, M., Onder, I., Secer, A., Yusuf, A., Sulaiman, T.A., Bayram, M., Aydin, H.: The analytical solutions of Zoomeron equation via extended rational sin-cos and sinh-cosh methods. Phys. Scr. **96**(9), 094002 (2021). https://doi.org/10.1088/1402-4896/ac0374

Cinar, M., Secer, A., Bayram, M.: An application of Genocchi wavelets for solving the fractional Rosenau-Hyman equation. Alex. Eng. J. **60**(6), 5331–5340 (2021). https://doi.org/10.1016/j.aej.2021.04.037

Cinar, M., Onder, I., Secer, A., Yusuf, A., Sulaiman, T.A., Bayram, M., Aydin, H.: The analytical solutions of zoomeron equation via extended rational sin-cos and sinh-cosh methods. Phys. Scr. **96**(9), 094002 (2021). https://doi.org/10.1088/1402-4896/ac0374

Dutta, H., Günerhan, H., Ali, K.K., Yilmazer, R.: Exact Soliton Solutions to the Cubic-Quartic Non-linear Schrödinger Equation With Conformable Derivative. Front. Phys. (2020). https://doi.org/10.3389/FPHY.2020.00062

Ekici, M., Mirzazadeh, M., Sonmezoglu, A., Zhou, Q., Moshokoa, S.P., Biswas, A., Belic, M.: Dark and singular optical solitons with kundu-eckhaus equation by extended trial equation method and extended g'/g-expansion scheme. Optik **127**(22), 10490–10497 (2016). https://doi.org/10.1016/j.ijleo.2016.08.074

Ekici, M., Zhou, Q., Sonmezoglu, A., Moshokoa, S.P., Ullah, M.Z., Biswas, A., Belic, M.: Solitons in magneto-optic waveguides by extended trial function scheme. Superlattices Microstruct. **107**, 197–218 (2017). https://doi.org/10.1016/J.SPMI.2017.04.021

Esen, H., Ozdemir, N., Secer, A., Bayram, M.: On solitary wave solutions for the perturbed Chen-Lee-Liu equation via an analytical approach. Optik **245**, 167641 (2021). https://doi.org/10.1016/J.IJLEO.2021.167641

Gonzalez-Gaxiola, O., Biswas, A., Yildirim, Y., Moraru, L.: Highly dispersive optical solitons in birefringent fibers with polynomial law of nonlinear refractive index by laplace-adomian decomposition. Mathematics (2022). https://doi.org/10.3390/math10091589

Guner, O.: Shock waves solution of nonlinear partial differential equation system by using the ansatz method. Optik **130**, 448–454 (2017). https://doi.org/10.1016/j.ijleo.2016.10.076

Guzel, N., Bayram, M.: Numerical solution of differential-algebraic equations with index-2. Appl. Math. Comput. **174**(2), 1279–1289 (2006). https://doi.org/10.1016/j.amc.2005.05.035

Kudryashov, N.A.: Optical solitons of mathematical model with arbitrary refractive index. Optik **224**, 165391 (2020). https://doi.org/10.1016/j.ijleo.2020.165391

Li, L., Wei, B., Yang, Q., Ge, D.: Auxiliary differential equation finite-element time-domain method for electromagnetic analysis of dispersive media. Optik **184**, 189–196 (2019). https://doi.org/10.1016/j.ijleo.2019.03.057

Liu, W., Zhang, Y., Luan, Z., Zhou, Q., Mirzazadeh, M., Ekici, M., Biswas, A.: Dromion-like soliton interactions for nonlinear schrödinger equation with variable coefficients in inhomogeneous optical fibers. Nonlinear Dyn. (2019). https://doi.org/10.1007/s11071-019-04817-w

Liu, S., Zhou, Q., Biswas, A., Liu, W.: Phase-shift controlling of three solitons in dispersion-decreasing fibers. Nonlinear Dynamics **98**(1), 395–401 (2019). https://doi.org/10.1007/S11071-019-05200-5

Mahak, N., Akram, G.: Extension of rational sine-cosine and rational sinh-cosh techniques to extract solutions for the perturbed NLSE with Kerr law nonlinearity. Eur. Phys. J. Plus **134**(4), 1–10 (2019). https://doi.org/10.1140/epjp/i2019-12545-x

Mahak, N., Akram, G.: Exact solitary wave solutions by extended rational sine-cosine and extended rational sinh-cosh techniques. Phys. Scr. **94**(11), 115212 (2019). https://doi.org/10.1088/1402-4896/ab20f3

Mirzazadeh, M., Ekici, M., Zhou, Q., Biswas, A.: Exact solitons to generalized resonant dispersive nonlinear schrödinger's equation with power law nonlinearity. Optik **130**, 178–183 (2017). https://doi.org/10.1016/j.ijleo.2016.11.036

Ozdemir, N., Esen, H., Secer, A., Bayram, M., Sulaiman, T.A., Yusuf, A., Aydin, H.: Optical solitons and other solutions to the Radhakrishnan-Kundu-Lakshmanan equation. Optik **242**, 167363 (2021). https://doi.org/10.1016/J.IJLEO.2021.167363

Ozisik, M., Secer, A., Bayram, M., Aydin, H.: An encyclopedia of kudryashov's integrability approaches applicable to optoelectronic devices. Optik **265**, 169499 (2022). https://doi.org/10.1016/j.ijleo.2022.169499

Ozisik, M., Cinar, M., Secer, A., Bayram, M.: Optical solitons with Kudryashov's sextic power-law nonlinearity. Optik **261**, 169202 (2022). https://doi.org/10.1016/j.ijleo.2022.169202

Qiao, N., Zou, B.: Nonlocal orientation diffusion partial differential equation model for optics image denoising. Optik **124**(14), 1889–1891 (2013). https://doi.org/10.1016/j.ijleo.2012.05.034

Raslan, K.R., Ali, K.K., Shallal, M.A.: The modified extended tanh method with the Riccati equation for solving the space-time fractional EW and MEW equations. Chaos Solitons Fract. **103**, 404–409 (2017). https://doi.org/10.1016/j.chaos.2017.06.029

Ren, X., Wang, J., Ren, G., Zhai, J., Tan, Y., Yang, X.: Solving the differential equation of light rays in Cartesian coordinates. Optik **194**, 163055 (2019). https://doi.org/10.1016/j.ijleo.2019.163055

Samir, I., Badra, N., Seadawy, A.R., Ahmed, H.M., Arnous, A.H.: Exact wave solutions of the fourth order non-linear partial differential equation of optical fiber pulses by using different methods. Optik **230**, 166313 (2021). https://doi.org/10.1016/j.ijleo.2021.166313

Secer, A., Cinar, M.: A Jacobi wavelet collocation method for fractional fisher's equation in time. Therm. Sci. **24**(Suppl. 1), 119–129 (2020)

Srivastava, H.M., Günerhan, H., Ghanbari, B.: Exact traveling wave solutions for resonance nonlinear Schrödinger equation with intermodal dispersions and the Kerr law nonlinearity. Math. Methods Appl. Sci. **42**(18), 7210–7221 (2019). https://doi.org/10.1002/MMA.5827

Srivastava, H.M., Baleanu, D., Machado, J.A.T., Osman, M.S., Rezazadeh, H., Arshed, S., Günerhan, H.: Traveling wave solutions to nonlinear directional couplers by modified Kudryashov method. Phys. Scr. **95**(7), 075217 (2020). https://doi.org/10.1088/1402-4896/AB95AF

Taghizadeh, N., Mirzazadeh, M.: The modified extended Tanh method with the Riccati Equation for solving nonlinear partial differential equations. Math. Aeterna **2**(2), 145–153 (2012)

Yildirim, Y., Biswas, A., Guggilla, P., Khan, S., Alshehri, H., Belić, M.: Optical solitons in fibre bragg gratings with third- and fourth-order dispersive reflectivities. Ukr. J. Phys. Opt. **22**, 239–254 (2021). https://doi.org/10.3116/16091833/22/4/239/2021

Yildirim, Y., Biswas, A., Dakova-Mollova, A., Guggilla, P., Khan, S., Alshehri, H., Belić, M.: Cubic-quartic optical solitons having quadratic-cubic nonlinearity by sine-gordon equation approach. Ukr. J. Phys. Opt. **22**, 255–269 (2021). https://doi.org/10.3116/16091833/22/4/255/2021

Yıldırım, Y., Biswas, A., Khan, S., Mahmood, M., Alshehri, H.: Highly dispersive optical soliton perturbation with kudryashov's sextic-power law of nonlinear refractive index. Ukr. J. Phys. Opt. **23**(1), 24–29 (2022). https://doi.org/10.3116/16091833/23/1/24/2022

Zayed, E., Shohib, R., Alngar, M., Biswas, A., Ekici, M., Khan, S., Alzahrani, A., Belić, M.: Optical solitons and conservation laws associated with Kudryashov's sextic power-law nonlinearity of refractive index. Ukr. J. Phys. Opt. **22**, 38–49 (2021). https://doi.org/10.3116/16091833/22/1/38/2021

Zayed, E.M., Alngar, M.E., Biswas, A., Yıldırım, Y., Guggilla, P., Khan, S., Alzahrani, A.K., Belic, M.R.: Cubic-quartic optical soliton perturbation with lakshmanan-porsezian-daniel model. Optik **233**, 166385 (2021). https://doi.org/10.1016/j.ijleo.2021.166385